PAPER

Agricultural beneficial microbes accelerate soil degradation of poly(butylene adipate-*co*-terephthalate) (PBAT) films

Yuan He, [ab] Yun Huang,[a] Yi Dan,*[a] Long Jiang, [a] Hong Zhang, [b] Huan Liu[b] and Yanjiao Qi[b]

Three common agricultural beneficial microbes, *Trichoderma harzianum*, *Bacillus cereus*, and *Pseudomonas fluorescens*, were utilized as effective agents in enhancing the degradation of poly(butylene adipate-*co*-terephthalate) (PBAT) within a soil environment. All of microbes accelerated the degradation of PBAT. Under specific conditions(Tri15), the degradation rate of PBAT films at 360 days can achieve over 70%. Scanning electron microscopy (SEM) images show that the surface of PBAT films cracks after 360 days of exposure to these three specific microbes because of the degradation of the PBAT. Gel permeation chromatography (GPC) analysis reveals that in the presence of these microbes the PBAT undergoes progressive molar-mass reduction. The 16S rRNA sequencing analysis revealed a significant shift in the microbial community structure following the introduction of the beneficial microbial inoculants. Specifically, the relative abundances of *Alpha-proteobacteria* and *Beta-proteobacteria* were markedly enriched in the treatment groups. Concurrently, FTIR analysis indicated a decrease in the relative intensities of the ester C–O–C (at $\sim$1260 cm^{-1}) and carbonyl C=O (at $\sim$1710 cm^{-1}) absorption bands. These spectroscopic changes are associated with the cleavage of the polymer backbone. The co-occurrence of this specific bacterial enrichment with the observed chemical changes suggests a potential link between the introduced microbial consortium and the enhanced degradation process.

1 Introduction

Plastic mulch technology first emerged in the mid-20th century in Europe and Asia and has since been widely adopted in regions such as North America, Europe, South Asia, and Africa. Its application spans a variety of crops, from staple crops such as wheat and maize to high-value cash crops like fruits and vegetables.[1,2] In regions with underdeveloped agricultural infrastructure, this technology has significantly improved food security by enhancing crop yields.[3] These mulch films are mainly composed of polyethylene, a material with slow degradation rate. Initially, the harmful effects of polyethylene mulch on the environment were underestimated, resulting in an insufficient accumulation of recovered debris.[4] This issue eventually leads to serious pollution of residual mulch in certain regions,[5] which has a negative impact on soil structure, function and fertility, ultimately leading to a decrease in seed germination rate.[6] These adverse effects reduce crop quality and

pose a major challenge to sustainable agricultural development.[7]

Recently, the use of biodegradable polymeric materials as alternatives to polyethylene in plastic mulch films has received widespread attention.[8] PBAT has emerged as a promising candidate in the agricultural sector due to its excellent extensibility, elongation, heat resistance, and impact strength.[9,10] Furthermore, the global production of PBAT had increased substantially, rising from 11 900 metric tons in 2011 to 33 800 metric tons in 2018, accounting for approximately 7.2% of the global bio-plastics output.[11,12] However, the degradation of PBAT mulch under actual field conditions has proven to be considerably slower than ideal.[13] For example, Wu *et al.* observed only superficial minor fissures on PBAT mulch after 180 days in cotton cultivation, while Wang *et al.* reported a mere 2.3% degradation rate in farmland soil over three months. This slow *in situ* degradation can be largely attributed to suboptimal environmental temperatures, which fall below the optimal range for both hydrolytic and microbial activity, thereby significantly limiting the degradation rate.[14–17] It is crucial that the degradation of PBAT films occurs at a controlled rate; premature degradation resulting in the loss of essential water retention and thermal regulation functions, leading to film disintegration during critical stages of plant growth.[18,19] Given

[a]State Key Laboratory of Polymer Materials Engineering of China (Sichuan University), Polymer Research Institute of Sichuan University, Chengdu 610065, China. E-mail: danyi@scu.edu.cn; jianglong@scu.edu.cn

[b]Gansu Province Research Center for Basic Sciences of Surface and Interface Chemistry, College of Chemical Engineering, Northwest Minzu University, Lanzhou 730124, China

these considerations, there is an urgent need to identify effective microbial strains that can optimize degradation of PBAT mulch film in agricultural settings.[20–22] Current research focuses on various microbial strains extract from soil with the potential to degrade PBAT which inherently possess PBAT-degrading ability.[23,24] A more efficient PBAT degrader, *Stenotrophomonas* sp. YCJ1 isolated from farmland soil showed 10.14 mass% of PBAT degradation at 37 °C for 5 days.[25] However, the methods by which the microbial strains are isolated from soil present challenges in the separation and reproduction of microbes, thereby restricting the scalability of production processes.[26]

Agricultural beneficial microbes represent a category of commercial microbial agents employed in agricultural production to diminish pest infestations and to enhance crop yields.[27] As a commercially available and mature microbial inoculant, the product has been demonstrated to possess a satisfactory biosafety profile through long-term application and environmental monitoring.[28,29] In this study, these three common agricultural beneficial microbes will be used to improve the degradation of polybutylene adipate-*co*-terephthalate (PBAT) in the soil environment. Compared with isolating and scaling native degraders, commercially available inoculants are easier to source and may be lower cost. For instance, traditional PCR-based methods require an upfront investment of thousands of dollars in equipment alone. In contrast, commercially formulated beneficial microbes are readily available as agricultural inputs, being a practical and feasible protocol to improve PBAT degradation.[30–32] Scanning electron microscopy, Fourier transform infrared spectroscopy and gel permeation chromatography will be employed to investigate the degradation-promoting effects of the three microbes on degrading PBAT under different concentration conditions, and then 16S rDNA gene sequencing will be utilized to assess the impact of introducing these beneficial agricultural strains on soil microbiome composition and diversity, unveiling underlying mechanisms by which they exert effects, aiming at establishing a simpler method of promoting the degradation of PBAT films in agricultural environments.

2 Materials and methods

2.1 Materials

The PBAT (FLEX-262, $M(—)_n$: 3.92×10^4: $M(—)_w/M(—)_n$: 1.679) with the chemical structure depicted in Scheme 1 was purchased from Guangzhou Kingfa Science and Technology Co., Ltd.

The experimental soil samples were collected from the upper layer of arable land in Binzhou, Shandong, located at coordinates 37.22 °N latitude and 118.02 °E longitude. The soil was characterized as a sandy loam. The initial soil composition was
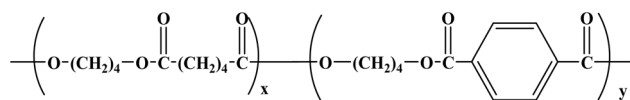
characterized by an organic matter content of 7.43 g kg^{-1}, total nitrogen content of 0.590 g kg^{-1}, moisture content of 32.7%, and a pH value of 6.8. After that, the soil was dried in a vacuum oven at 80 °C for 8 hours and subsequently sieved through a 10-mesh (2 mm) sieve to eliminate plant debris, stones, and other extraneous materials. This treatment effectively standardized the initial moisture while substantially reducing the native microbial background (Table S1) without significantly altering soil physicochemical properties.[33–35]

The agricultural beneficial microbes used in this study comprised *Bacillus cereus* (Bac), *Trichoderma harzianum* (Tri), and *Pseudomonas fluorescens* (Flu). The Bac and Tri strains were supplied by Bates Co. Ltd, and the Flu strain was obtained from Shandong Tainol Pharmaceutical Co. Ltd. According to the manufacturer's specifications, each formulation contained a mixture of spores and vegetative cells, with declared viable counts of 3×10^8 CFU g^{-1} for Tri, 8×10^8 CFU g^{-1} for Bac, and 5×10^8 CFU g^{-1} for Flu. The dry matter content of the powdered inoculants, as determined by drying at 105 °C to constant weight, was 90% for Tri, 91% for Bac, 93% for Flu. All microbial preparations were stored at 4 °C prior to use. Each microbial strain was applied individually without co-cultivation.

2.2 Degradation test of PBAT films by the agricultural beneficial microbes

The PBAT was first subjected to vacuum drying at 80 °C for 8 hours to eliminate moisture. Subsequently, a PBAT film with a thickness of 500 ± 20 μm was prepared through hot pressing at 230 °C under a pressure of 10 MPa. The enhanced mechanical integrity of the thicker films was crucial to ensure their complete retrieval and handling over multiple sampling intervals without premature fragmentation. This approach guaranteed the reliability of successive mass loss measurements and spectroscopic analyses on the same set of samples, thereby allowing for a robust and quantitative comparison of the efficacy of different microbial treatments. The thermal stability of the polymer under these conditions was verified by DSC, which showed no significant change in the material's thermal properties before and after processing (Fig. S1).

500.0 ± 0.2 g of soil was placed into experimental vessels. Specified amounts of each powdered inoculant (30 ± 0.1, 150 ± 0.1, 450 ± 0.1, and 900 ± 0.1 g) were directly suspended in ultrapure water and thoroughly mixed into the soil. These amounts corresponded to nominal mass concentrations of 1%, 5%, 15%, and 30% (w/w). Based on this, all experimental samples were designated as Tri1, Tri5, Tri15, Tri30, Bac1, Bac5, Bac15, Bac30, Flu1, Flu5, Flu15, and Flu30, where the prefix indicates the microbial strain (*Trichoderma*, *Bacillus cereus*, or *Pseudomonas fluorescens*) and the suffix indicates the nominal mass concentration. The corresponding absolute dosing values for viable cells (CFU g^{-1} dry soil) and microbial biomass (g dry weight g^{-1} dry soil) for each of these samples are provided in Table 1. This setup involved a single inoculation at day 0, with no further re-inoculation, to evaluate the long-term efficacy of the microbes from a one-time application.

Scheme 1 Chemical structure of PBAT.

© 2025 The Author(s). Published by the Royal Society of Chemistry

Table 1 Absolute dosing of beneficial microbes in the soil degradation experiment

Designate	m (g^{-1} dry soil)	CFU (g^{-1} dry soil)	g dry weight (g^{-1} dry soil)
Tri1	$(1 \pm 0.01) \times 10^{-2}$ g	$(3 \pm 0.03) \times 10^{6}$	$(0.9 \pm 0.01) \times 10^{-2}$ g
Tri5	$(5 \pm 0.01) \times 10^{-2}$ g	$(1.5 \pm 0.03) \times 10^{7}$	$(4.5 \pm 0.01) \times 10^{-2}$ g
Tri15	$(1.5 \pm 0.01) \times 10^{-1}$ g	$(4.5 \pm 0.03) \times 10^{7}$	$(1.35 \pm 0.01) \times 10^{-1}$ g
Tri30	$(3 \pm 0.01) \times 10^{-1}$ g	$(9 \pm 0.03) \times 10^{7}$	$(2.7 \pm 0.01) \times 10^{-1}$ g
Bac1	$(1 \pm 0.01) \times 10^{-2}$ g	$(8 \pm 0.05) \times 10^{6}$	$(0.91 \pm 0.01) \times 10^{-2}$ g
Bac5	$(5 \pm 0.01) \times 10^{-2}$ g	$(4 \pm 0.05) \times 10^{7}$	$(4.55 \pm 0.01) \times 10^{-2}$ g
Bac15	$(1.5 \pm 0.01) \times 10^{-1}$ g	$(1.2 \pm 0.05) \times 10^{8}$	$(1.365 \pm 0.01) \times 10^{-1}$ g
Bac30	$(3 \pm 0.01) \times 10^{-1}$ g	$(2.4 \pm 0.05) \times 10^{8}$	$(2.73 \pm 0.01) \times 10^{-1}$ g
Flu1	$(1 \pm 0.01) \times 10^{-2}$ g	$(5 \pm 0.05) \times 10^{6}$	$(0.93 \pm 0.01) \times 10^{-2}$ g
Flu5	$(5 \pm 0.01) \times 10^{-2}$ g	$(2.5 \pm 0.05) \times 10^{7}$	$(4.65 \pm 0.01) \times 10^{-2}$ g
Flu15	$(1.5 \pm 0.01) \times 10^{-1}$ g	$(7.5 \pm 0.05) \times 10^{7}$	$(1.395 \pm 0.01) \times 10^{-1}$ g
Flu30	$(3 \pm 0.01) \times 10^{-1}$ g	$(1.5 \pm 0.05) \times 10^{8}$	$(2.79 \pm 0.01) \times 10^{-1}$ g

The entire 360-day burial experiment was conducted under controlled laboratory ambient conditions in Chengdu, Sichuan Province. The temperature was not artificially controlled and thus reflected typical indoor seasonal fluctuations. The soil vessels were kept under indoor ambient light with a natural day/night cycle but were shielded from direct sunlight. Aeration was maintained passively through the design of the vessels, which featured a loosely fitted lid and a 10 cm headspace above the soil, allowing for gas exchange while conserving moisture.

The survival and colonization potential of the introduced beneficial microbes were assessed for the experimental samples described above (*i.e.*, soils treated with samples Tri1, Tri5, Tri15, Tri30, Bac1, Bac5, Bac15, Bac30, Flu1, Flu5, Flu15, and Flu30). Soil samples were destructively collected at 0, 7, and 21 days post-inoculation. The abundance of viable cells for each specific strain was determined by serial dilution and plate counting on selective media: *Bacillus cereus* and *Pseudomonas fluorescens* on Nutrient Agar, and *Trichoderma harzianum* on Potato Dextrose Agar supplemented with chloramphenicol. The results confirmed that all inoculated strains successfully established and maintained viable populations across the tested concentrations, validating the feasibility of this approach (Table S2).

The pre-conditioned square PBAT film samples (thickness: 0.5 mm, side length: 4 cm) were placed at a uniform depth of 5 cm below the soil surface. Each soil sample accommodated four individual film pieces, ensuring that the films neither contacted one another nor overlapped. No microbial strains (Blank) were introduced into the soil in the control experiment. Each trial was repeated three times to ensure accuracy and reliability.

The experimental duration was extended over 360 days, with observations conducted bi-weekly. The soil moisture content was maintained at the target level of 30% (by weight), which was monitored and adjusted at bi-weekly intervals using a handheld soil moisture meter by replenishing with sterile ultrapure water.

The corresponding PBAT films were carefully extracted at predetermined intervals of 90, 180, 270 and 360 days, and their surfaces were cleaned with ethanol for subsequent analysis of surface morphology, average molecular weight, crystallinity, and other significant parameters. The experimental protocol is depicted in Scheme 2 below.

2.3 Measurement of the degradation rate of PBAT film

After retrieval from the soil, PBAT films were processed using a standardized cleaning protocol to ensure comparability. The samples were carefully retrieved, immersed in 70% aqueous ethanol for 30 minutes to terminate biological activity and remove soluble contaminants, and subsequently rinsed three times with ultrapure water. The cleaned films were then dried at 60 °C until constant mass was achieved. To assess potential mass loss attributable to the cleaning process itself, control
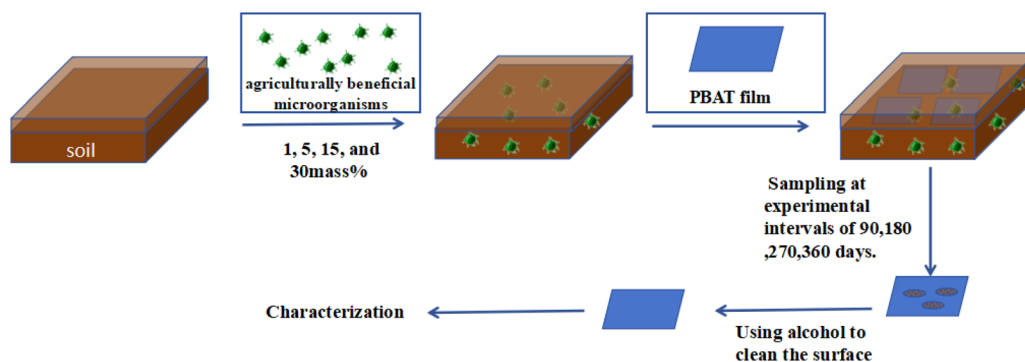
Scheme 2 Degradation test of PBAT films by the microbes.

experiments were conducted using pristine PBAT films. These films underwent the identical cleaning procedure, yielding a mass recovery rate of 99.2 ± 0.5%. This result confirms the minimal impact of the cleaning protocol on film mass. All mass measurements were performed in triplicate, with data presented as mean ± standard deviation.

Then, the degradation rate (D) was calculated by eqn (1):

$$D = \frac{m_0 - m_t}{m_0} \times 100\% \qquad (1)$$

where m_0 and m_t represent the mass of the initial PBAT film and the PBAT film after t days of degradation, respectively.

2.4 Characterization

The morphology of the PBAT films after various degradation periods was observed by scanning electron microscopy (SEM) with a Phenom G2 ProX scanning electron microscope (Netherlands). Prior to observation, the PBAT films were coated with gold, and the test voltage was set at 10 kV. The SEM images were acquired at an accelerating voltage of 5 kV and a working distance of 8 mm under high vacuum conditions.

The molecular structure was characterized by Fourier transform infrared (FT-IR) spectroscopy using a Nicolet iS10 instrument (Thermo Fisher Scientific Inc., USA), covering the frequency range of 4000 to 400 cm^{-1} with a resolution of 4 cm^{-1}. Fourier-transform infrared (FTIR) spectroscopy analysis was conducted using a spectrometer equipped with an ATR accessory. An automatic baseline correction was applied to all collected spectra.

The average molecular weight and molecular weight distribution of PBAT were comprehensively analyzed by gel permeation chromatography (GPC, Waters, USA), equipped with a Waters 1515 pump and a Waters 2414 refractive index detector. Samples were prepared by dissolving 2 mg of polymer in 1 mL chloroform for 12 hours, followed by triple filtration through 0.45 μm nylon membranes. Analysis used 25 μL injections with a micro-syringe. The PBAT concentration was precisely maintained at 2 mg mL^{-1}, with tetrahydrofuran (THF) as the mobile phase at a flow rate of 1 mL min^{-1}. The measurements were performed at 35 °C.Calibration employed narrow polystyrene standards, with reported molecular weights being relative approximations due to hydrodynamic volume differences between polystyrene and polyeste to analysis allowed monitoring of changes in molecular weight and molecular weight distribution resulting from microbial degradation.

Library Preparation, and Sequencing Genomic DNA was extracted from soil samples using the MOBIO PowerSoil DNA Isolation Kit. The V3–V4 hypervariable region of the bacterial 16S rRNA gene was amplified with primers 357F and 806R-1-8. Sequencing libraries were prepared following the standard Illumina two-step amplicon PCR protocol, and paired-end sequencing (2 × 250 bp) was performed on an Illumina NovaSeq platform using the NovaSeq 6000 SP 500 Cycle Reagent Kit -1. Bioinformatic analysis was primarily conducted with the UPARSE pipeline and mothur software -3. Raw sequence reads were demultiplexed, quality-filtered using Trimmomatic (v0.35), and

primers were trimmed with cutadapt (v1.16). Paired-end reads were merged using FLASH (v1.2.11). Subsequent filtering removed sequences with ambiguities, those shorter than 200 bp or longer than 485 bp, and sequences with homopolymer runs exceeding 8 bp. High-quality sequences were clustered into Operational Taxonomic Units (OTUs) at a 97% identity threshold, and chimeric sequences as well as singleton OTUs were removed. Taxonomy was assigned against the SILVA 128 database using mothur's classify.seqs command with a confidence threshold of 0.6–3. Statistical Analysis Microbial community analysis was performed in the R environment (v3.6.3). Alpha diversity was estimated using the Shannon, Simpson, Chao1, and ACE indices. Beta diversity was calculated based on Bray–Curtis, Jaccard, and weighted/unweighted UniFrac distances, and visualized *via* Principal Coordinate Analysis (PCoA) and Non-metric Multidimensional Scaling (NMDS). The significance of group differences in beta diversity was tested using Analysis of Similarities (ANOSIM). Differential abundance of taxa between groups was identified using Linear Discriminant Analysis Effect Size (LEfSe), with a significance threshold of $p < 0.05$ and a log 10 LDA score $\geq$ 2.0^{-3}.

Fungal mycelia were isolated from soil samples and subjected to genomic DNA extraction using the cetyltrimethylammonium bromide (CTAB) method −9. The extracted DNA was purified and its quality was verified by 0.8% agarose gel electrophoresis, with concentration and purity assessed using a NanoDrop spectrophotometer (A260/A280 ratios ~1.8) −2. The internal transcribed spacer (ITS) region was amplified by polymerase chain reaction (PCR) with universal fungal primers ITS1-F (5′-CTTGGTCATTTAGAGGAAGTAA-3′) and ITS4 (5′-TCCTCCGCTTATTGATATGC-3′) -2. The 50 μL PCR reaction mixture contained 1× PCR buffer, 200 μM dNTPs, 0.2 μM of each primer, 1 U Taq DNA polymerase, and 50 ng template DNA. Amplification was performed under the following conditions: initial denaturation at 94 °C for 5 min; 35 cycles of 94 °C for 30 s, 55 °C for 30 s, and 72 °C for 1 min; final extension at 72 °C for 7 min. The PCR products were purified and sequenced bidirectionally using the BigDye Terminator v3.1 Cycle Sequencing Kit on a 3730xl DNA Analyzer -2-5.

The viability of the introduced microbial inoculants in soil was monitored over time using a plate count method. Soil samples were collected at 0, 7, and 21 days after inoculation. Serial dilutions of the soil suspensions were prepared and plated. Specifically, nutrient agar and potato dextrose agar were used as the non-selective media for bacteria and fungi, respectively. All platings were performed in triplicate, and the results are presented as mean values. Statistical analysis (ANOVA, $p < 0.05$) confirmed that no significant decrease in viable cell numbers occurred over the 21-day period. The complete dataset is provided in the SI data.

3 Results and discussion

3.1 Effects of the three microbes on the degradation of PBAT films

The effect of the addition of three microbes on the degradation of PBAT films was evaluated according to the degradation rate

of PBAT films. The degradation rates of PBAT films at different microbesl mass concentrations were systematically investigated, and the results are presented in Fig. 1 and Tables S3–S6.

All PBAT films exhibit some degree of mass loss over time, indicating continuous degradation. However, none of the films achieved complete (100%) degradation within 360 days, and the degradation process is ongoing. The addition of the three microbesl strains enhance the degradation of PBAT films, showing that the slopes of curves of the PBAT with added microbes are all larger than that of the control sample named blank.[36] And the enhancement in degrading rate varies with degrading time. At 90 days, the addition of the microbesl strains result in a modest increase in degradation compared to the control sample (Blank). It is worth noting that PBAT films usually undergo more degradation after 180 days due to the influence of the strain. This timeline is consistent with the typical growth period of most crops, reflecting the potential applicability of this method in the agricultural environment.

Furthermore, different microbesl strains exhibit different promotion to the degradation at different concentrations. At a concentration of 1%, the enhancement effect of all three microbes is minimal. When the concentration increases to 5%, *Trichoderma harzianum* (Tri) and *Pseudomonas fluorescens* (Flu) both show a significant promotion to PBAT degradation. At 15%, the degradation rates of PBAT films by Tri, *Bacillus cereus*

(Bac), and Flu reach 70.02%, 64.53%, and 48.23%, respectively, while the Blank sample is only 17.13%. When the concentration further increases to 30%, the degradation rate of PBAT films by Flu increases significantly. For Tri and Bac, with the concentrations increasing from 15% to 30%, degradation rates of the correspond PBAT films decrease by 30.01% and 8.21%, respectively. The results suggest that increasing the microbesl concentration within a certain range could accelerate the degradation of PBAT films, more than 15% of the concentration would have different effects on the degradation for the different microbes, indicating that the higher microbesl content does not necessarily lead to a greater degradation enhancement. The specific reasons will continue to be analyzed in Section 3.5.

This study employed 0.5 mm thick PBAT films to provide a controlled system for evaluating microbial degradation. We acknowledge that this thickness does not directly replicate field conditions and likely influences degradation kinetics, including mass transfer limitations and biofilm formation dynamics. Consequently, the absolute degradation rates reported here should not be directly extrapolated to predict the in-service lifetime of commercial mulch films. Instead, our findings provide critical comparative and mechanistic insights into the intrinsic capabilities of the tested microbial strains. Future work employing standard-thickness films is the essential next step to validate these promising results under more field-realistic conditions.
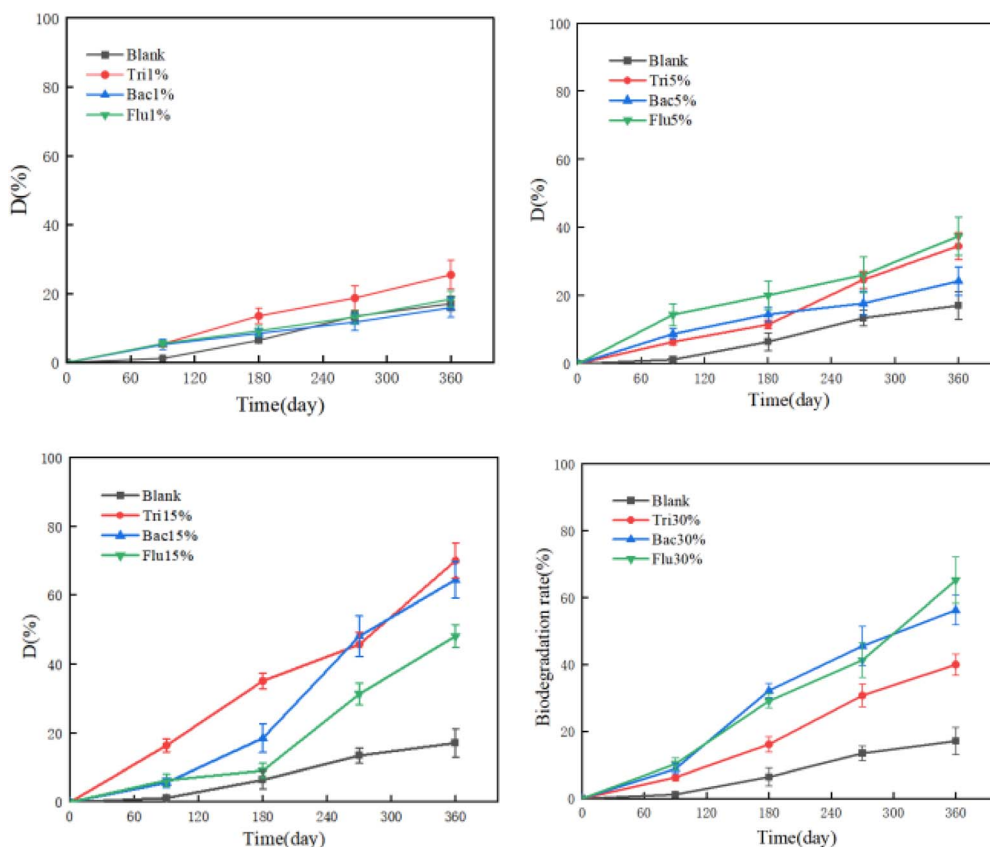

Fig. 1 Variation of degradation rate (*D*) of PBAT films as influenced by different microbes at different mass concentrations over time. Data points represent the mean ± SD (*n* = 3). Different lowercase letters at the same time point indicate statistically significant differences among treatments (*p* < 0.05). (Blank: without microbes; Bac: *Bacillus cereus*; Tri: *Trichoderma harzianum*; Flu: *Pseudomonas fluorescens*).

3.2 The change of morphology of the PBAT films with different microbes

Following the degradation test, mold spots, cracks, and fragmentations were observed on the surface of the PBAT films, indicating the occurrence of degradation.[37] The macroscopic morphology photos (Fig. 2-photo) and the scanning electron microscopy images (Fig. 2-SEM) further illustrate the effects of microbesl species and its content on the degradation of PBAT films. These results are presented in Fig. 2 and S2–S4.

Before degradation, PBAT films display a characteristic white, opaque appearance, accompanied by a smooth, crack-free surface. SEM images corroborate the presence of relatively flat, crack-free, and mildew-free surfaces. As the experiment progresses, non-inoculated samples display an increase in surface roughness and a loss of gloss, despite no significant additional changes being detected. In contrast, the inoculated film samples undergo noticeable yellowish-brown discoloration with clear cracking and breakage, indicating that all three microbesl strains significantly enhance the degradation of PBAT.[38] The extent of degradation varies with the type of microbesl strain and its content.

Trichoderma harzianum primarily induces rupture in the PBAT. At a concentration of 15%, it exhibits the most substantial promotion to PBAT degradation, resulting in severe rupture. However, when the concentration increases to 30%, the degree of film rupture decreases, and the surface microbesl colonies become more prominent. *Bacillus cereus* promotes visible mold growth and cracking on the PBAT film surfaces. At a concentration of 5%, the degradation mainly manifests as localized colonies with minimal cracks. As the concentration increases to 15%, these colonies rapidly expand over time, eventually covering the entire film surface and leading to visible degradation. SEM observations reveal distinct fungal growth and extensive cracking. However, when the concentration further increases to 30%, the time of colony formation is slightly advanced, the overall degradation is reduced. *Pseudomonas fluorescens* causes noticeable microbesl and fungal blooms on the PBAT film surfaces, although no obvious rupture is observed, the phenomenon is only detectable under SEM. At a low concentration of 1%, the films exhibit a yellowish tinge, and microbesl growth is observable under the microscope. As the concentration increases, the number of microbesl spots on the film surface significantly increases, and mycelial growth becomes more apparent in electron microscope images.
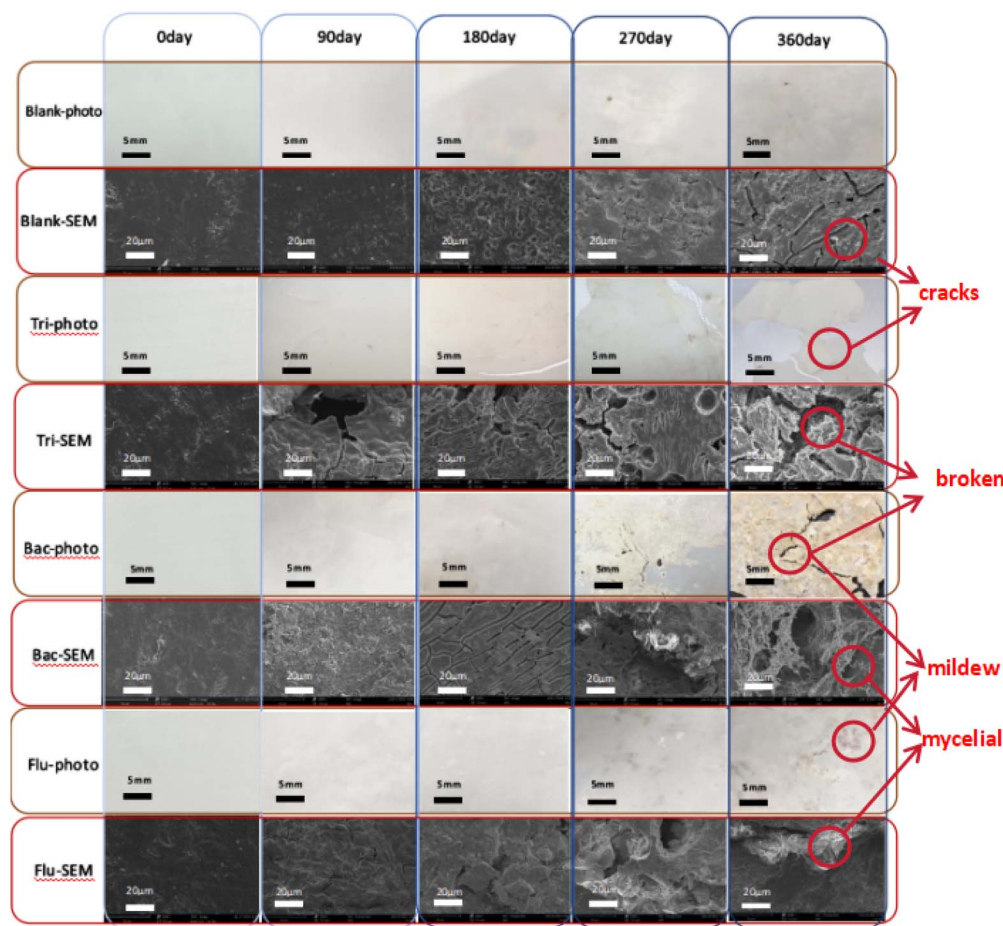

Fig. 2 Macroscopic morphology photos (-photo) and scanning electron microscopy images (-SEM) of PBAT films after the degradation test at different time points, under the influence of three different microbes with a concentration of 15% by mass, respectively.

Despite the varying degrees of PBAT degradation promoted by the three strains, all PBAT films exhibit a trend of that the degradation increases with time. At 90 days, no significant surface changes are observed in the PBAT films under microbesl influence. By 180 days, however, surface cracks and stains begin to emerge, becoming more pronounced over time, with samples displaying severe cracking and mold growth by 360 days. Microscopically, the microstructure of the samples progressively deteriorates over time. Degradation initially occurs at isolated locations and subsequently spread to other areas. This deterioration is attributed to hydrolytic and microbial activities in the soil environment, which trigger the disintegration of PBAT ester linkages, leading to fragmentation of polymer into smaller molecules. SEM images reveal abundant pores, indicating surface-level degradation. The increase in pore quantity correlates with higher material loss rates and more advanced degradation. Mycelial growth is clearly observed in the samples, as evidenced in the figures. These changes in surface morphology correspond with the previously observed degradation rate results. The degradation of PBAT films is primarily attributed by microorganism adhesion, which is a localized and gradual process. Further studies are necessary to elucidate the specific degradation-promoting mechanisms of the three microbesl strains on PBAT.

3.3 Average molecular weight and its distribution of PBAT after degradation for different time under the influence of the three microbes

The degradation of PBAT is evidenced by a significant reduction in mass and in formation of mold holes, likely resulting from alterations in the molecular structure.[39] Given that all the three microbesl strains effectively promote PBAT degrading at a mass concentration of 15%, the average molecular weight and distribution of PBAT under the action of the microbesl at this concentration were analyzed by GPC. The results are presented in Fig. 3 and Table 2.

As illustrated in Fig. 3, the main peak in the GPC profile gradually shifts to the right as the PBAT films degradation experiment progressed. Degradation test of PBAT films by the agricultural beneficial microbes progresses, signifying a reduction in the molecular weight of the sample over time. At the same time, the width of the main peak becomes wider, especially after 360 days of degradation, a relatively wide and smaller peak appears at the 18-minute of outflow time. The smaller peaks marked in Fig. 3 suggest the presence of a greater number of components with reduced molecular weight, indicating ongoing of the degradation.[40] Data listed in Table 2 shows that as the degradation time increases, the average molecular weight of PBAT decreases, and the molecular weight distribution becomes wider. These changes correspond with the results
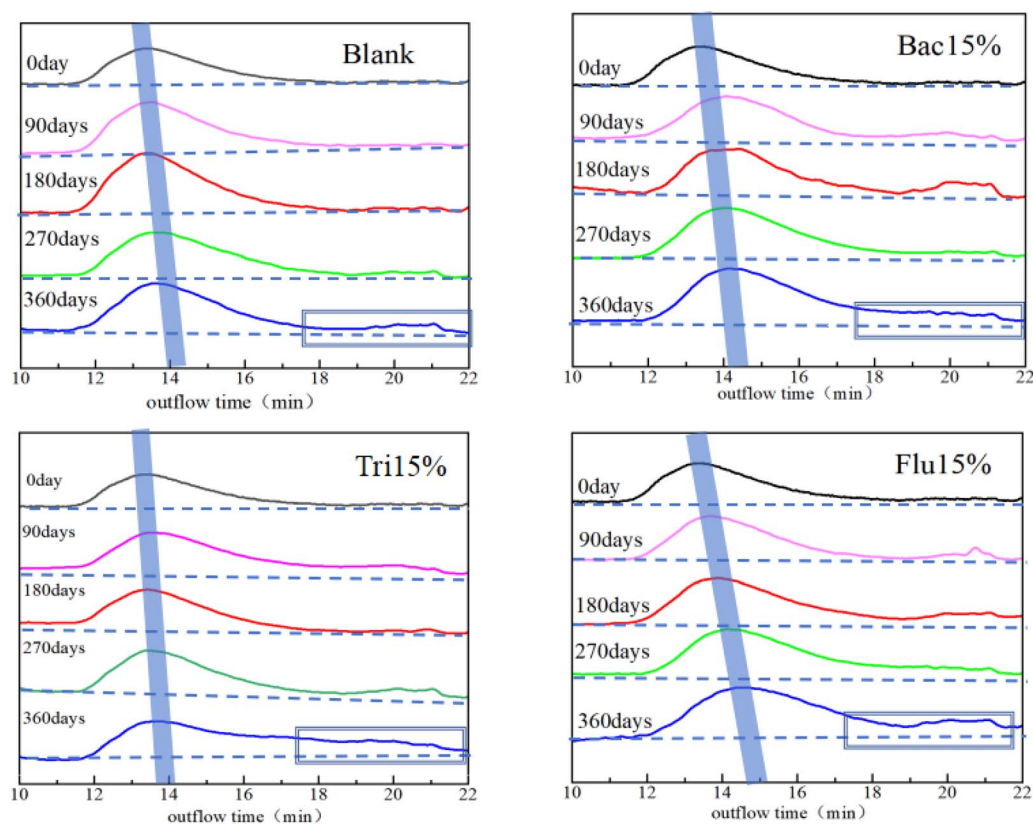

Fig. 3 Elution curves of PBAT after degradation for different time under the influence of the three microbes at a concentration of 15% by mass, respectively. (Blank: without microbes; Bac 15%: with microbes Bac of 15% mass concentration; Tri 15%: with microbes Tri of 15% mass concentration; Flu 15%: with microbes Flu of 15% mass concentration).

Table 2 Average molecular weight and its distribution of PBAT after degradation for different time under the influence of the three microbes at a concentration of 15% by mass

Sample	Degradation time (day)	$M(—)_n$ ($\times 10^4$)	$M(—)_w$ ($\times 10^4$)	PDI
Blank	0	3.92 ± 0.02	6.58 ± 0.02	1.68 ± 0.02
	90	3.83 ± 0.02	6.61 ± 0.03	1.73 ± 0.02
	180	3.31 ± 0.02	6.42 ± 0.03	1.94 ± 0.02
	270	3.16 ± 0.02	6.51 ± 0.02	2.06 ± 0.02
	360	1.57 ± 0.01	6.35 ± 0.02	4.05 ± 0.01
Flu 15%	90	3.02 ± 0.02	6.73 ± 0.03	2.23 ± 0.02
	180	3.02 ± 0.02	6.60 ± 0.02	2.18 ± 0.02
	270	0.32 ± 0.01	6.13 ± 0.03	18.76 ± 0.05
	360	0.31 ± 0.02	6.02 ± 0.04	19.16 ± 0.05
Tri 15%	90	3.02 ± 0.02	6.19 ± 0.03	2.05 ± 0.02
	180	2.19 ± 0.02	4.14 ± 0.02	1.89 ± 0.02
	270	0.46 ± 0.01	6.74 ± 0.03	14.83 ± 0.05
	360	0.58 ± 0.01	6.98 ± 0.04	11.97 ± 0.05
Bac 15%	90	3.20 ± 0.02	6.42 ± 0.02	2.03 ± 0.02
	180	1.60 ± 0.02	5.79 ± 0.02	3.62 ± 0.03
	270	1.41 ± 0.01	6.58 ± 0.02	4.68 ± 0.03
	360	0.54 ± 0.01	5.87 ± 0.04	10.81 ± 0.05

previously observed in degradation rates and morphological transformations. The degradation process is initiated at the contact points, with alterations in the molecular weight distribution being more obvious than the decrease in molecular weight itself. This observation indicates that the degradation maybe does not occur as a simultaneous rupture of the entire polymer chain but rather a partial and gradual process.

As shown in Fig. 3 and Table 2, compared with the blank sample, the addition of the three strains accelerates the production of components with smaller molecular weight, suggesting that the microbesl strains indeed promote the degradation of PBAT. Different microbes has different promotion to the degradation of PBAT. *Bacillus cereus* (Bac) makes the production of components with smaller molecular weight at 90 days of the degradation experiment, with a significant broadening of the peak by 360 days. *Trichoderma harzianum* (Tri) shows comparable results with the Bac at a same concentration. The components with smaller molecular weight become obvious at 90 days, and as time went on, the molecular weight further decreases and the molecular weight distribution becomes wider, though the promoting effect of Tri is not as obvious as that of Bac. Among the three microbes, *Pseudomonas fluorescens* (Flu) induces the most significant shift in the main peak and the most increase in the components with smaller molecular weight, suggesting that, among the three microbes, the Flu should have the most significant effect on the degradation of PBAT.[41]

3.4 Analysis of Fourier infrared spectroscopy of the PBAT films with different microbes

The structural changes in PBAT films following degradation were further investigated by Fourier transform infrared spectroscopy (FTIR), and the results are presented in Fig. 4, where the microbesl concentration is 15% by mass. The FTIR spectra of other PBAT films subjected to microbes with concentration of 1%, 5%, and 30% by mass are provided in Fig. S5–S7.

As depicted in Fig. 4, the initial PBAT film exhibits characteristic absorption peaks at 1710 cm^{-1} and 1265 cm^{-1}. The peak at 1710 cm^{-1} corresponds to the stretching vibration of the ester carbonyl (C=O) groups, while the peak at 1265 cm^{-1} belongs to the C–O groups linked to the benzene ring within the PBAT structure.[43] After degradation, the peaks at 1710 cm^{-1} and 1265 cm^{-1} gradually decrease with the prolongation of burial time, up to 360 days, indicating that the C–O and C=O bonds are cleaved during the degradation process. Additionally, new absorption peaks emerge at 3290 cm^{-1}, corresponding to –OH functional groups. Compared with the blank sample, the microbes-treated samples show earlier appearance of the peaks of –OH functional groups in the 3290 cm^{-1} regions and a larger peak area. The C–O and C=O peaks of 1710 cm^{-1} and 1265 cm^{-1} decrease more rapidly and distinctly in these samples. This suggests that the three microbesl strains significantly enhance the degradation of PBAT at a 15% mass concentration. In the microbesl treatment, the C–O and C=O peaks of the samples treated with Bac decrease most significantly, and these peaks almost disappear completely after 360 days. And the samples treated with Flu display the second-most substantial effect, whereas those treated with Tri show the least structural alteration.

Fig. S5–S7 reveals that the structural changes of the PBAT varies with concentrations of the added microbesl strains, though the general trend aligns with the results of degradation rate and morphological characterization. The PBAT sample treated with Flu. Shows structural alterations with an increasing promotional effect as concentration rises, peaking at a 30% of the concentration. In contrast, the PBAT sample treated with Bac. Shows the most significant structural changes at a concentration of 15%. This finding aligns with earlier morphological observations, though there is a slight deviation from the degradation rate data, which suggests that Tri-treated samples undergo more obvious degradation. However, the FTIR data indicate that the most substantial degradation occurs in
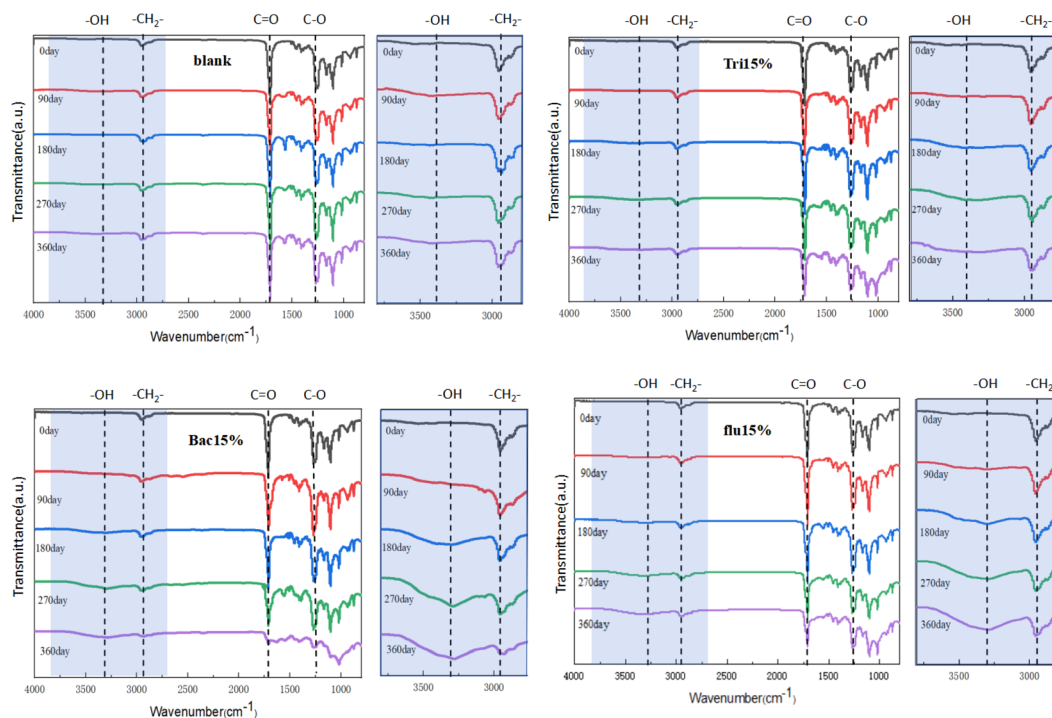
Fig. 4 FTIR spectra of PBAT films after degradation for different time under the action of different microbes (Blank: without microbes; Bac 15%: with microbes Bac of 15% mass concentration; Tri 15%: with microbes Tri of 15% mass concentration; Flu 15%: with microbes Flu of 15% mass concentration).

Bac-treated samples. This discrepancy may be due to the fact that the degradation rate primarily reflects overall changes in the film, while FTIR spectra insights into local structural changes. The result suggests that the PBAT degradation maybe initiated at a localized level and then gradually developed.

3.5 Impact of the microbesl addition on soil microbial community

Using PBAT in the terrestrial ecosystem triggers a complex interaction between the polymer and the indigenous microbial consortium, including both microbesl and fungal communities.[42] These microorganisms initiate the formation of a biofilm on the PBAT surface. This process promotes the gradual disintegration of PBAT into smaller molecular entities. The diversity and abundance of microbial populations play a crucial role in determining the degradation rate of PBAT, and the significant differences in degradation potential have been observed among different microbial groups.[43]

Previous experimental results have demonstrated that the addition of all three microbesl strains enhances the degradation of PBAT, although the extent of this enhancement varies depending on the microbesl concentration. Flu exhibits a greater promoting effect as concentration increases, while Tri shows the most obvious degradation-promoting effect at a mass concentration of 15%. To further investigate the mechanism underlying these observations, it is essential to examine the influence of these microbesl strains on the soil microbial community in greater detail.

16S rRNA gene sequencing is here utilized to evaluate the changes of soil microbiome after introducing the three different beneficial microbes, and the results of comparison of the microbial community composition are shown in Fig. 5 and S8.

The comparative analysis of the initial soil samples and the blank soil samples without beneficial microbes shows that only the insertion of PBAT film has little effect on the soil microbial community. The introduction of the three agricultural microbesl strains result in soil microbes community composition significant shifts. Furthermore, the addition of beneficial microbes leads to the proliferation of specific soil components Notably, the components of *Alphaproteomicrobes* and *Betaproteomicrobes* show a remarkable increase with addition of beneficial microbes, although changing trends are not consistent as three beneficial microbes added. In fact, the maximum improvement of *Alphaproteomicrobes* and *Betaproteomicrobes* appears at the addition quantity of 30% mass concentration of *Bacillus cereus* and *Pseudomonas fluorescens* (the maximum additive amount in the experiments), while the addition quantity of 15% mass concentration of *Trichoderma harzianum* confirmes the best efficient. The results are consistent with that of the aforementioned degradation experiments.

Comparing these findings with the previous results on the effects of beneficial microbes content and diversity on PBAT degradation, it can be seen that the primary catalytic effect is not directly attributed by the beneficial microbes themselves. Instead, due to the introduction of beneficial microbes, the increase in the number of *Alphaproteomicrobes* and *Betaproteomicrobes* mainly promotes the degradation of PBAT. To
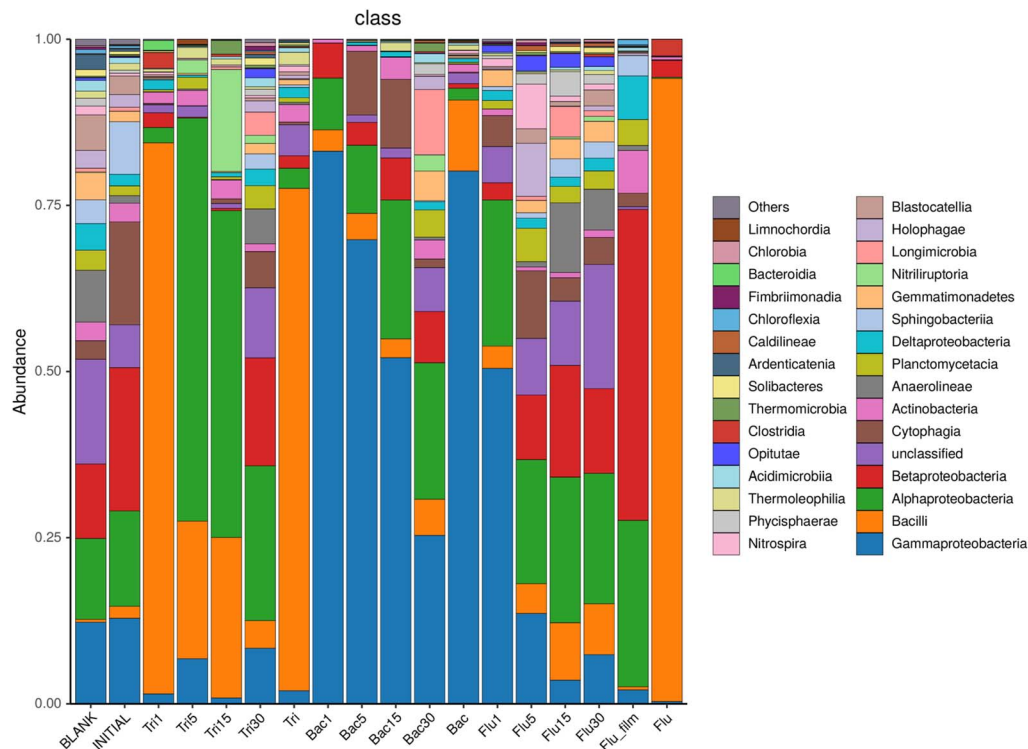
Fig. 5 Soil microbes community composition and relative abundance at class level after PBAT films degradation under the action of different microbes by R16s. (Initial: the PBAT film before degradation; blank: without microbes; Bac, Tri, and Flu are the experimental microbes; Bac1– Bac30: with microbes Bac of 1–30% mass concentration; Tri1–Tri30: with microbes Tri of 1–30% mass concentration; Flu 1–30: with microbes Flu of 1–30% mass concentration).

corroborate this proposition, the microbial community structure on the surface of the PBAT film was further examined, and the results indicate that the main microbial species are also *Alphaproteomicrobes* and *Betaproteomicrobes*. It is likely that *Alphaproteobacteria* and *Betaproteobacteria* are among the dominant microbial groups colonizing the film's surface.

From the analysis of the sequential changes of microbesl communities after the introduction of microbes into the soil, similar results are obtained. As shown in Fig. S8, compared to the initial soil samples, the content of *rhizobiales* and *burkholderiales* in the blank samples increase insignificantly. After adding the beneficial microbes, the abundance of these two groups of microbes increases significantly, being related to the degree of PBAT degradation affected by microbesl concentration. The result suggests that the increase of *rhizobiales* and *burkholderiales* in soil maybe facilitates the degradation of PBAT film.

These findings highlight that the enhancement of PBAT degradation by these three strains is not due to their intrinsic degradation ability, but due to their different effects on soil microbial communities when introduced at different concentrations. This in turn promotes the degradation of PBAT.

To evaluate the impact of the fungal inoculant (*Trichoderma harzianum*) on the soil microbiome, ITS sequencing was conducted. The results are shown in Fig. 6 and S9.

Comparative analysis of fungal community structure through ITS sequencing revealed a pattern consistent with the
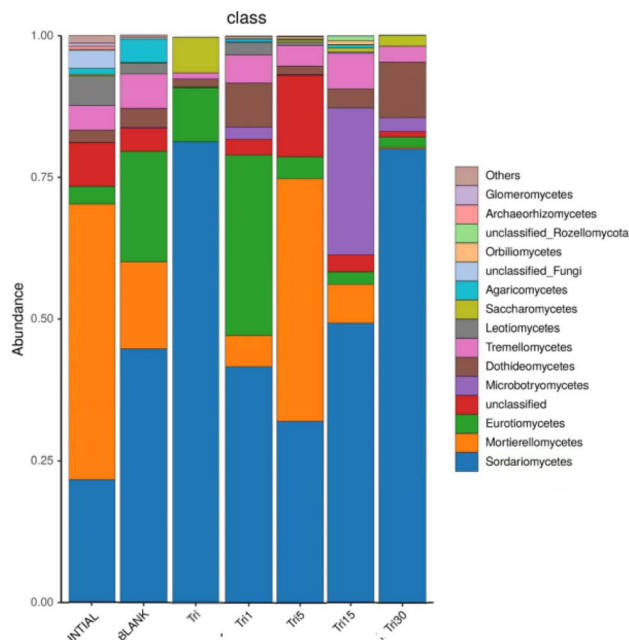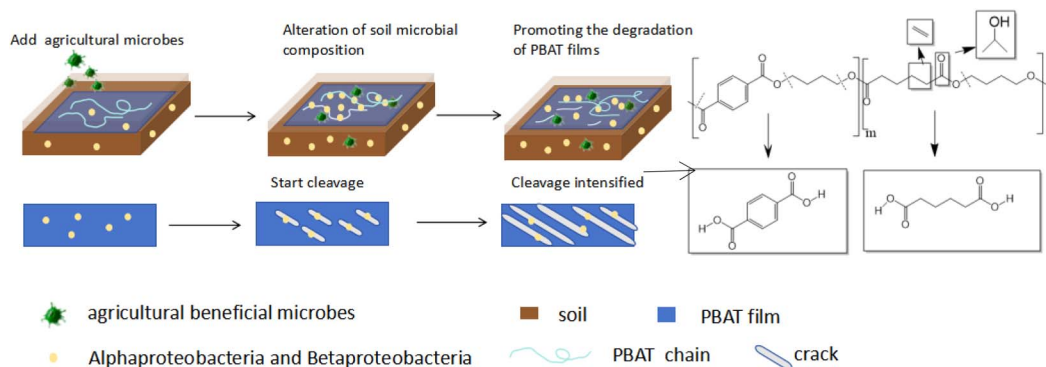

Fig. 6 Soil microbes community composition and relative abundance at class level after PBAT films degradation by ITS. (Initial: the PBAT film before degradation; blank: without microbes; Tri1–Tri30: with microbes Tri of 1–30% mass concentration).

Scheme 3 Proposed conceptual model.

bacterial data. While the introduced *Trichoderma harzianum* successfully colonized the soil, its direct relative abundance in the community remained moderate. Notably, a significant enrichment was observed in specific native fungal classes, particularly *Micrebotryomycetes* and *Dothideomycetes*, following the introduction of the Tri inoculant. This suggests that the fungal inoculant's role extends beyond its direct metabolic activity, potentially triggering a restructuring of the resident fungal assemblage. This coordinated shift in both microbial kingdoms indicates that the enhanced PBAT degradation results from a synergistic maybe response within the broader soil microbiome, rather than from the direct action of any single introduced strain. The convergence of these community-level responses across different microbial domains underscores the ecological complexity underlying the biodegradation process.

3.6 The degradation process of PBAT films by microbes

Basing on the results of the above analyses, the degradation process proposed conceptual model of PBAT films by the microbes is schematically presented in Scheme 3.

Initially, the addition of microbes altered the composition of the soil microbial community, leading to an increased abundance of *Alphaproteobacteria* and *Betaproteobacteria*, which are considered potential key players in the PBAT degradation process. Secondly, the PBAT film degradation proceeded in a gradual and localized manner. We hypothesize that this was due to the non-uniform distribution and growth of the introduced microbial consortia in the soil. This heterogeneous colonization could have led to enhanced degradation at specific contact points, resulting in the observed surface features like biofilms and cracks. The combination of FTIR data—suggesting cleavage of C–O and C=O bonds and formation of C–H and O–H bonds—together with observed physical erosion, supports a model of localized and progressive PBAT degradation in the presence of the three microbes.

4 Conclusions

Agricultural beneficial microbes, *Trichoderma harzianum*, *Bacillus cereus*, and *Pseudomonas fluorescens*, can change the soil

microbial community, enhance the cleavage of carbon–oxygen bonds and carbonyl groups in PBAT and promote the degradation of PBAT film under the soil environments. All the three microbes with a mass concentration of 15% are capable of inducing significant degradation of PBAT, chieving up to >70% mass loss (Tri15) after 360 days under microcosm conditions; effects were bacterium- and dose-dependent. Introducing agricultural beneficial microbes into the soil environments is an efficient and feasible strategy of accelerating degradation of PBAT. Compared to the microorganisms found in soil the easily obtained and less expensive of the used microbes makes the established method in the study be a more straightforward and feasible for promoting degradation of PBAT, holding significant potential application in the bioremediation of PBAT to reduce pollution of residue mulch films and packaging materials.

Our results demonstrate a clear correlation between the inoculation of beneficial microbes, the enrichment of specific bacterial taxa (*e.g.*, *Alpha/Beta-proteobacteria*), and the chemical degradation of PBAT, it is important to note that these findings do not establish a direct mechanistic causality. The observed community shifts and polymer breakdown could be influenced by complex biotic and abiotic interactions within the soil microenvironment. While these controlled laboratory conditions establish important proof-of-concept, we recognize the need for further validation under realistic field conditions. Future work will therefore focus on translating these findings to agricultural settings using standard-thickness mulch films, while continuing to investigate the underlying enzymatic mechanisms. This combined approach will be crucial for developing effective microbial-assisted degradation strategies for plastic waste in real farming environments.

Conflicts of interest

There are no conflicts to declare.

Data availability

The data supporting this article have been included as part of the supplementary information (SI). Supplementary information is available. See DOI: https://doi.org/10.1039/d5ra06589e.

Acknowledgements

References

1 F. Pedra, M. L. Inácio, P. Fareleira, et al., Long-Term Effects of Plastic Mulch in a Sandy Loam Soil Used to Cultivate Blueberry in Southern Portugal, *Pollutants*, 2024, **4**(1), 16–25.

2 S. X Li, Z. H. Wang, S. Q. Li, Y. J. Gao and X. H. Tian, Effect of Plastic Sheet Mulch, Wheat Straw Mulch, and Maize Growth on Water Loss by Evaporation in Dryland Areas of China, *Agric. Water Manage.*, 2013, **116**, 39–49.

3 H. Zhang, C. Miles, B. Gerdeman, et al., Plastic mulch use in perennial fruit cropping systems – A Review, *Sci. Hortic.*, 2021, **281**, 109975.

4 C. Zhang, X. Liu, L. Zhang, et al., Assessing the aging and environmental implications of polyethylene mulch films in agricultural Land, *Environ. Sci.: Processes Impacts*, 2024, **26**(8), 1310–1321.

5 H. Liu, X. Yang, G. Liu, C. Liang, S. Xue, H. Chen, C. J. Ritsema and V. Geissen, Response of soil dissolved organic matter to microplastic addition in Chinese loess soil, *Chemosphere*, 2017, **185**, 907–917.

6 X. Zou, W. Niu, J. Liu, et al., Effects of Residual Mulch Film on the Growth and Fruit Quality of Tomato (Lycopersicon esculentum Mill.), *Water, Air, Soil Pollut.*, 2017, **228**(2), 71.

7 K. Wang, W. Min, M. Flury, et al., Impact of Long-term conventional and biodegradable film mulching on microplastic abundance, soil structure and organic carbon in a cotton Field, *Environ. Pollut.*, 2024, **356**, 124367.

8 K. Candlen, C. Conrad, P. Prommart, et al., Biodegradable Poly(butylene adipate-co-terephthalate)/Poly(lactic) Acid Mulch Film with Soy Waste Filler for Improved Biodegradation and Plant Growth, *Adv. Energy Sustain. Res.*, 2025, **6**(9), 250068.

9 M. Velandia, K. L. DeLong, A. Wszelaki, et al., Use of Polyethylene and Plastic Biodegradable Mulches among Tennessee Fruit and Vegetable Growers, *HortTechnology*, 2020, **30**(2), 212–218.

10 T. Zhang, C. Zhang, X. Song and Y. Weng, Progress in preparation and application of PBAT thin films, *China Plast.*, 2021, **35**, 115–125.

11 Y. Cui, J. Wei, L. Gou, C. Han, Y. Han, J. Zhu, K. Liu and Y. Xie, Shule County 2021 fully biodegradable plastic film test demonstration and appropriate promotion and application, *Agric. Technol. Equip.*, 2022, **5**, 44–46.

12 Y. Ma, A. Zhang, J. Yang and J. Ren, Preparation and properties of PBAT, *Plastics*, 2010, **39**, 98–101.

13 N. R. Nair, V. C. Sekhar, K. M. Nampoothiri and A. Pandey, Biodegradation of Biopolymers, *Biodegradation of Biopolymers Chapter*, 2019, (02), 738–755.

14 R. Wufuer, W. Li, S. Wang, et al., Isolation and degradation characteristics of PBAT film degrading microbes, *Int. Res. J. Publ. Environ. Health*, 2022, **19**(24), 17087.

15 D. Griffin-LaHue, S. Ghimire, Y. Yu, et al., In-field degradation of soil-biodegradable plastic mulch films in a Mediterranean Climate, *Sci. Total Environ.*, 2022, **806**, 150238.

16 R. Qi, D. L. Jones, Q. Liu, et al., Field test on the biodegradation of poly(butylene adipate-co-terephthalate) based mulch films in Soil, *Polym. Test.*, 2021, **93**, 107009.

17 P. Rizzarelli and G. Impallomeni, Evidence for Selective Hydrolysis of Aliphatic Copolyesters Induced by Lipase Catalysis, *Biomacromolecules*, 2004, (5), 433–444.

18 Z. Liu, Z. Li, J. Jiang, et al., Biodegradable and Multifunctional PBAT/Lignin Mulch Films for Green Agriculture, *ACS Appl. Polym. Mater.*, 2025, **7**(16), 10711–10720.

19 H. Wang, D. Wei, A. Zheng and H. Xiao, Soil burial biodegradation of antimicrobial biodegradable PBAT films, *Polym. Degrad. Stab.*, 2015, **116**, 14–22.

20 M. Sander, Biodegradation of Polymeric Mulch Films in Agricultural Soils:Concepts,Knowledge Gaps and Future Research Directions, *Environ. Sci. Technol.*, 2019, (23), 04–15.

21 F. Trinh Tan, D. G. Cooper, M. Maric and J. A. Nicell, Biodegradation of a synthetic co-polyester by aerobic mesophilic microorganisms, *Polym. Degrad. Stab.*, 2008, **93**, 1479–1485.

22 H. Jia, M. Zhang, Y. Weng, et al., Degradation of poly (butylene adipate-co-terephthalate) by Stenotrophomonas sp. YCJ1 isolated from farmland soil, *J. Environ. Sci.*, 2021, **103**, 50–58.

23 G. Chhetri, J.-M. Jeon, G. Hwang, et al., Biodegradation of PCL, PBS, and PBAT at low temperatures by Aeromicrobium sp. JJY06: A newly isolated strain for cold-environment plastic Cleanup, *J. Hazard. Mater.*, 2025, **495**, 138896.

24 J. Y. Cho, et al., Novel Poly(butylene adipate-co-terephthalate)-degrading Bacillus sp. JY35 from wastewater sludge and its broad degradation of various bioplastics, *Waste Manage.*, 2022, **144**, 1–10.

25 H. Jia, M. Zhang, Y. Weng, et al., Degradation of poly(butyleneadipate-co-terephthalate) by Stenotrophomonas sp. YCJ1 isolated from farmland Soil, *J. Environ. Sci.*, 2021, **103**, 50–58.

26 A. Kanwal, M. Zhang and F. Sharaf, Screening of poly (butylene adipate-co-terephthalate) PBAT co-polyesters hydrolyzing bacteria from Soil, *Polym. Bull.*, 2023, **81**(3), 2407–2428.

27 R. Chaudhary, A. Nawaz, Z. Khattak, et al., Microbial Bio-control agents: A comprehensive analysis on sustainable pest management in Agriculture, *J. Agric. Food Res.*, 2024, **18**, 101421.

28 C. F. Chukwuneme, A. S. Ayangbenro, et al., Potential innovations from the application of beneficial soil microbes to promote sustainable crop production, *Stud. Univ. Babes-Bolyai. Biol.*, 2024, **69**(1), 51–86.

29 C. F. Chukwuneme, A. S. Ayangbenro, *et al.*, Potential innovations from the application of beneficial soil microbes to promote sustainable crop production, *Stud. Univ. Babes-Bolyai. Biol.*, 2024, **69**(1), 51–86.

30 X. Huo, Y. Gao, Q. Lin, J. Zeng, T. Zhang, M. Chu, H. Yang, Y. Shi, B. Wang, J. Sun, *et al.*, Isolation and identification of poly (butylene adipate-co-terephthalate)-degrading microbes, *Xinjiang Agric. Sci.*, 2017, **54**, 2086–2091.

31 R. Kumar, B. Farda, A. Mignini, *et al.*, Microbial Solutions in Agriculture: Enhancing Soil Health and Resilience Through Bio-Inoculants and Bioremediation, *Bacteria*, 2025, **4**(3), 28.

32 K. Gutiérrez-Moreno, A. I. Olguín-Martínez, A. C. Montoya-Martínez, *et al.*, Trichoderma in Sustainable Agriculture and the Challenges Related to Its Effectiveness, *Diversity*, 2025, **17**(10), 734.

33 J. Schroeder, L. Kammann, M. Helfrich, *et al.*, Impact of common sample Pre-treatments on key soil microbial Properties, *Soil Biol. Biochem.*, 2021, **160**, 108321.

34 P. Marschner and B. Zheng, Direction and magnitude of the change in water content between two periods influence soil respiration, microbial biomass and nutrient availability which can be modified by intermittent air-Drying, *Soil Biol. Biochem.*, 2022, **166**, 108559.

35 L. Philippot, C. Chenu, A. Kappler, *et al.*, The interplay between microbial communities and soil Properties, *Nat. Rev. Microbiol.*, 2023, **22**(4), 226–239.

36 R. Qi, D. L. Jones, Q. Liu, *et al.*, Field test on the biodegradation of poly (butylene adipate-co-terephthalate) based mulch films in soil, *Polym. Test.*, 2021, **93**, 107009.

37 J. Liu, L. Hou, T. Liu, P. Wang, X. Gao and Y. Lin, Isolation of PBAT plastic-degrading microbes and their degradation characteristics, *J. Agro-Environ. Sci.*, 2021, **40**, 129–136.

38 J. Hao, Z. Min and W. Yunxuan, Degradation of polylactic acid/polybutylene adipate-co-terephthalate by coculture of Pseudomonas mendocina and Actinomucor elegans, *J. Hazard. Mater.*, 2021, **403**, 123679.

39 R. Herrera, L. Franco, A. Rodríguez-Galán, *et al.*, Characterization and degradation behavior of poly (butylene adipate-co-terephthalate) s, *J. Polym. Sci., Part A: Polym. Chem.*, 2002, **40**(23), 4141–4157.

40 P. Cui, J. Wang, L. Mao, *et al.*, Investigation of biodegradable microparticle release and environmental accumulation in Poly(butylene succinate) degradation under UV and non-UV aging Conditions, *Polym. Degrad. Stab.*, 2025, **237**, 111323.

41 C. QIAO, W. YANG, Z. LI, *et al.*, Experimental teaching reform of polymer molar mass determination using gel permeation chromatography coupled with light Scattering, *Chin. J. Chromatogr.*, 2024, **42**(8), 812–818.

42 Z. Hua, Y. Li, X. He, *et al.*, Quantitative analysis of PBAT microplastics and their degradation products in soil by mass Spectrometry, *Eco-Environ. Health*, 2025, **4**(3), 100166.

43 M. Zhang, H. Jia, Y. X. Weng and C. T. Li, Biodegradable PLA/PBAT mulch on microbial community structure in different soils, *Int. Biodeterior. Biodegrad.*, 2019, **145**, 104817.